Received: 12 April 2019 | Revised: 1 July 2019 | Accepted: 14 August 2019

DOI: 10.4218/etrij.2019-0199

ORIGINAL ARTICLE

ETRI Journal WILEY

Blind symbol timing offset estimation for offset-QPSK modulated signals

Sushant Kumar | **Sudhan Majhi**

Department of Electrical Engineering, Indian Institute of Technology, Patna, India

Correspondence
Sushant Kumar, Department of Electrical Engineering, Indian Institute of Technology, Patna, India.
Email: sushant.pee15@iitp.ac.in

In this paper, a blind symbol timing offset (STO) estimation method is proposed for offset quadrature phase-shift keying (OQPSK) modulated signals, which also works for other linearly modulated signals (LMS) such as binary-PSK, QPSK, π/4-QPSK, and minimum-shift keying. There are various methods available for blind STO estimation of LMS; however, none work in the case of OQPSK modulated signals. The popular cyclic correlation method fails to estimate STO for OQPSK signals, as the offset present between the in-phase (I) and quadrature (Q) components causes the cyclic peak to disappear at the symbol rate frequency. In the proposed method, a set of close and approximate offsets is used to compensate the offset between the I and Q components of the received OQPSK signal. The STO in the time domain is represented as a phase in the cyclic frequency domain. The STO is therefore calculated by obtaining the phase of the cyclic peak at the symbol rate frequency. The method is validated through extensive theoretical study, simulation, and testbed implementation. The proposed estimation method exhibits robust performance in the presence of unknown carrier phase offset and frequency offset.

KEYWORDS

blind symbol timing offset estimation, cyclic correlation, linearly modulated signal, testbed validation

1 | INTRODUCTION

Blind estimation of the symbol timing offset (STO) for linearly modulated signals (LMS) has drawn significant attention owing to its potential applications in imminent wireless communication, where high spectrum efficiency is mandatory. The technology includes software defined radio, long-term evolution, and blind synchronization and parameter estimation of high-speed distributed networks, where the signal parameters must be estimated without any training sequences. Several methods have been introduced to improve the spectral efficiency [1–3]. Consequently, blind estimation has equal importance in high-speed communication systems where training sequences lose their correlation properties owing to a severe channel condition [4,5].

Offset quadrature phase-shift keying (OQPSK) is a variant of QPSK, in which the information stream of the in-phase (I) component is delayed by half of the symbol time from that of the quadrature (Q) component [6]. As a consequence, an OQPSK signal shows a maximum envelope change of 3 dB (70%) compared to the 100% change for QPSK. Practically, an OQPSK modulated signal has many advantages over QPSK because of its simplified power amplifier design [7]. The OQPSK modulation scheme is commonly used in high-speed wireless data transmission systems, especially terrestrial mobile communication

systems, wideband satellite communication systems, digital video broadcasting systems, and various other systems [8–10].

The STO estimation is widely categorized into two basic groups. The first group belongs to the data-aided group [11–14], which is not bandwidth efficient, as it uses a pilot signal or training sequences for the STO estimation. The second approach is the non-data–aided structure, which exploits the statistics of the received signal for the estimation, and is also known as blind estimation [13,15]. Some of the non-data–aided classical STO estimations are the early-late gate algorithm [16–18], Mueller and Muller algorithm [19], and Gardner algorithm [20,21].

A cyclostationarity approach proposed by Oerder and Meyr in [22] shows significant improvement in STO estimation. It exploits the cyclostationarity nature of the linear modulation signal and estimates the phase at the symbol rate. For the burst mode communications discussed in [23], two STO estimation methods are proposed. The first method utilizes the concept of maximum likelihood estimation. The second method is the extracting approach or tone filtering, which performs a squaring operation on the baseband signal [22]. A combined approach for finding the STO and frequency offset has been described in [24], which is based on the cyclostationarity approach but fails for OQPSK modulated signals. A symbol timing recovery algorithm for 16-quadrature amplitude modulation (16-QAM) has been proposed in [25], although the method performs well only at a high signal-to-noise ratio (SNR). An STO estimation method for PSK signals is discussed in [26], and also works in the high SNR regime. A joint frequency and timing offset estimation for minimum-shift keying (MSK) is presented in [27], where the MSK modulation is similar to the OQPSK. However, the method cannot be applied to OQPSK in a straightforward manner.

All of the aforementioned methods work only for non-offset modulations; only a few estimation algorithms have been proposed for OQPSK signals [28–30]. The joint phase and timing estimators for OQPSK using the ML method have been presented in [28,29]. They have considered a feedforward structure and oversampling of 2 and 4, respectively. Their performance is good for larger excess bandwidth, that is, $\beta \geq 0.5$; however, their accuracy deteriorates as β decreases.

To address the drawbacks of the available methods, a new blind STO estimation method is designed for OQPSK modulated signals that works even at low SNR and small excess bandwidth. The proposed method first compensates for the offset present between the I and Q components in an OQPSK signal and then exploits its cyclostationarity properties to extract the phase at the symbol rate frequency. The symbol rate frequency can be calculated by using the method described by Majhi and others in [1]. The performance of the proposed method is further upgraded with the help of an interpolation method. The proposed method is investigated through theoretical study, simulation, and testbed implementation.

Compared to the existing methods [28,29], the contributions of this paper are as follows:

- We propose an STO estimator which works for OQPSK along with other LMS such as BPSK, MSK, QPSK, and π/4-QPSK.
- The proposed method belongs to the blind estimation process, as it does not require any prior knowledge of the signal bandwidth, carrier phase, carrier frequency, or frequency offset.
- We propose a weighting function to obtain a weighted-cyclic spectrum (WCS) to enhance algorithm performance, especially for small excess bandwidth and low SNR.
- The proposed method shows robust performance in the presence of carrier phase offset and frequency offset.
- The experimental analysis in an indoor environment under flat fading channel demonstrates the efficacy of the proposed method.

The remainder of this paper is structured as follows. The signal and system model for single carrier transmission is reviewed in Section 2. Section 3 describes the proposed STO estimation and provides details of the cyclic cumulant and weighted cyclic cumulant. The performance of the proposed method through simulation and measurement results is evaluated in Section 4, followed by the conclusion in Section 5.

2 | SYSTEM MODEL

We assume that the received signals have cyclostationarity properties, which is a common feature in communications because of carrier modulation at the transmitter [31]. Practically, all unnatural signals characterize the cyclostationarity process, which can be easily analyzed with the help of a statistical tool discussed in [32]. In the majority of existing methods, the STO is estimated when the receiver has perfect knowledge regarding signal bandwidth and carrier frequency. However, we estimate the signal bandwidth and carrier frequency from the bandpass signal inspired by a blind process discussed in [33]. A baseband signal is achieved by down-converting the received bandpass signal [34].

The baseband received OQPSK signal with unknown timing and frequency offsets can be expressed in complex form as follows:

$$x(t) = e^{-j(2\pi f_o t+\phi)} \sum_{k=0}^{k-1} \Big(d_r[k] g(t-kT-\tau) + j d_i[k] g\Big(t-kT-\frac{T}{2}-\tau\Big)\Big) + w(t), \quad (1)$$

where ϕ is the carrier phase, f_o is the carrier frequency offset, K is the number of symbols, τ is the timing offset, and $d[k]=d_r[k]+jd_i[k]$ is the kth complex data symbol. T is the signal interval and $T/2$ is the timing offset between the I and Q components. When $T/2=0$, the imaginary part of the OQPSK signal defined in (1) becomes a QPSK signal. $w(t)$ is the additive white Gaussian noise having double-sided power spectral density with mean zero and variance σ_w^2. $g(t)$ is the received pulse shape given as $g(t)=h\tilde{g}(t)$, where h is the channel gain and $\tilde{g}(t)$ is a root raised cosine (RRC) filter with the parameter β, $0\le\beta\le 1$, applied as the roll-off factor. However, the proposed algorithm works for all pulse shaping filters. We assume the approximate bandwidth of $x(t)$ to be in the interval $[-(1+\beta)/2T,(1+\beta)/2T]$. Without loss of generality, the data symbol $d[k]$ is assumed to be independent and identically distributed (i.i.d) with mean of zero and variance ($E\{|d[k]|^2\}=1$).

A discrete time signal $x[n]$ is obtained after oversampling the received continuous time domain signal $x(t)$ by a factor P at a rate of P/T.

$$x[n]=e^{-j(2\pi f_o n+\phi)}\left(s_r[n]+js_i[n]\right)+w[n], \tag{2}$$

where $s_r[n]=\sum_{k=0}^{K-1} d_r[k]g[n-kP-N_\tau]$ and $s_i[n]=\sum_{k=0}^{K-1} d_i[k]g[n-kP-P/2-N_\tau]$ $\sum_{k=0}^{K-1} d_i[k]g[n-kP-P/2-N_\tau]$. The received signal $x[n]$ exhibits cyclostationarity properties for $P>4$ [35]. N_τ is the timing offset in terms of the number of samples related to τ. The oversampling factor is given as $P=T/T_s=F_s/f_s$, where $f_s=1/T$ is the symbol rate, F_s is the sampling rate, and $T_s=1/F_s$ is the sampling period, which is taken small enough so that intersymbol interference does not exist in the oversampled signal. In the case of a short-burst signal and high sampling rate, if f_s is a nonintegral multiple of F_s, then low frequency resolution is present, which degrades the estimation performance. To overcome these situations, the proposed method uses interpolation and zero padding techniques to improve the frequency resolution in addition to enhancing the performance of the STO estimation.

3 | SYMBOL TIMING OFFSET ESTIMATION

Blind STO estimation based on cyclostationarity properties is computationally more efficient and simpler than the nonlinear least square and ML methods. However, the existing cyclic correlation (CC) symbol timing offset estimation technique which would be a candidate for the proposed method fails for OQPSK signals. Therefore, we first provide justification as to why the CC method is not applicable to estimate STO in the case of OQPSK modulated signals. Afterward, a blind STO estimation algorithm is proposed for OQPSK, which also works for other LMS. The STO is estimated for BPSK, MSK, QPSK, $\pi/4$-QPSK, and OQPSK signals without having prior information regarding the modulation formats or parameters of the transmitted signal. The problem statement can be defined as: Estimate the STO of LMS $\{x[n]\}_1^N$ without any prior information regarding the signal parameters.

3.1 | Second-order cyclic spectrum of OQPSK signals

The second-order time-varying correlation function of the received complex baseband signal with zero time-lag can be expressed as follows:

$$c_{[x,2,1]}[n;0]=E\{x[n]x^*[n]\}. \tag{3}$$

The periodicity of the signal is extracted after applying the discrete Fourier transform (DFT) to (3). We can express the term $E\{x[n]x^*[n]\}$ as follows:

$$\begin{aligned}E\{x[n]x^*[n]\}=&E\left\{|s_r[n]|^2\right\}+E\left\{|s_i[n]|^2\right\}\\&+E\left\{|w[n]|^2\right\}.\end{aligned} \tag{4}$$

We derive the second-order time-varying correlation function of $s_r[n]$ as follows:

$$\begin{aligned}c_{[r]}[n;0]&=\sum_{k=0}^{K-1}\sum_{m=0}^{K-1}E\left\{d_r[k]d_r[m]\right\}g\left[n-kP-N_\tau\right]g\left[n-mP-N_\tau\right]\\&=\sigma_r^2\sum_{k=0}^{K-1}g^2\left[n-kP-N_\tau\right]\\&=\frac{\sigma_r^2}{P}\sum_{m=0}^{K-1}G\left[\frac{m}{P}\right]e^{j2\pi nm/P}e^{-j2\pi mN_\tau/P},\end{aligned} \tag{5}$$

where $G[\cdot]$ is the DFT of $g^2[\cdot]$, $\sigma_r^2=E[(d_r[k])^2]$, and the Poisson sum formula is applied to obtain the last equality. At the receiver, no RRC filter is present while estimating STO, so the receiver will not introduce any filter delay. The DFT of (5) can be obtained as follows:

$$\begin{aligned}C_{[r]}[\alpha;0]&=\frac{\sigma_r^2}{P}\sum_{n=0}^{K-1}\sum_{m=0}^{K-1}G\left[\frac{m}{P}\right]e^{-j2\pi n(\alpha-m/P)}e^{-j2\pi mN_\tau/P}\\&=\frac{\sigma_r^2}{P}\sum_{m=0}^{K-1}G\left[\frac{m}{P}\right]e^{-j2\pi mN_\tau/P}\delta\left[\alpha-\frac{m}{P}\right],\end{aligned} \tag{6}$$

where $\sum_{n=0}^{K-1}e^{-j2\pi n(\alpha-m/P)}=\delta[\alpha-m/P]$ for a large value of K, α represents the cyclic frequency, and $\sum_{n=0}^{K-1}e^{-j2\pi n(\alpha-m/P)}=\delta[\alpha-m/P]$ for a large value of K.

Similarly, we obtain the second-order cyclic spectrum of $s_i[n]$ as follows:

$$C_{[i]}[\alpha;0]=\frac{\sigma_i^2}{P}\sum_{m=0}^{K-1}G\left[\frac{m}{P}\right]e^{-j2\pi mN_\tau/P}e^{-j\pi m}\delta\left[\alpha-\frac{m}{P}\right]. \tag{7}$$

We have used a bandlimited filter at the receiver, $C_{[i]}[\alpha;0] \approx 0$ for $m > 1$. Therefore, we obtain the second-order cyclic spectrum of $x[n]$ by taking the DFT of $c_{[x]}[n;0]$ and apply bandlimiting for $m = 1$.

$$C_{[x,2,1]}[\alpha;0] = \frac{1}{P} G\left[\frac{1}{P}\right] e^{-j2\pi N_\tau/P} \left(\sigma_r^2 \delta\left[\alpha - \frac{1}{P}\right] - \sigma_i^2 \delta\left[\alpha - \frac{1}{P}\right]\right) + \sigma_w^2 \delta[\alpha], \tag{8}$$

Here, $\sigma_w^2 \delta[\alpha]$ is the cyclic spectrum of $w[n]$. We should obtain nonzero peaks of $C_{[x,2,1]}[\alpha;0]$ at $-1/P$, 0, and $1/P$ because of the bandwidth of the usual transmit filters [35]. However, $|C_{[x,2,1]}[\alpha;0]|$ yields maxima only at $\alpha = 1/P$ for the positive cyclic frequency. From (8), the cyclic spectrum function at $\alpha = 1/P$ is obtained as follows:

$$C_{[x,2,1]}[\alpha;0]|_{\alpha=1/P} = 0. \tag{9}$$

There is no cyclic peak at $\alpha = 1/P$ in (8), as the same-power I and Q cyclic components cancel each other out because of the presence of the $P/2$ offset between them. Therefore, this method fails in the case of an OQPSK modulated signal.

3.2 | Proposed method

We propose a second-order cyclic spectrum method for the estimation of STO in the case of OQPSK modulated signals. We observe from (8) that the cyclic spectrum yields a nonzero peak at $\alpha = 1/P$ if the I and Q components have a phase difference which is not equal to π, and that the peak is neither a local nor a global maxima. This peak is converted to a global maximum by making the phase difference zero between the I and Q components at $\alpha = 1/P$ and the roll-off factor is assumed to be large. However, the cyclic spectrum will not yield a global maximum at $\alpha = 1/P$ if the received SNR becomes low or the roll-off factor becomes small. In order to overcome this issue, a proper weighting approach is proposed to convert local maxima to global maxima when the phase difference is zero between the I and Q components at $\alpha = 1/P$, even for low SNR.

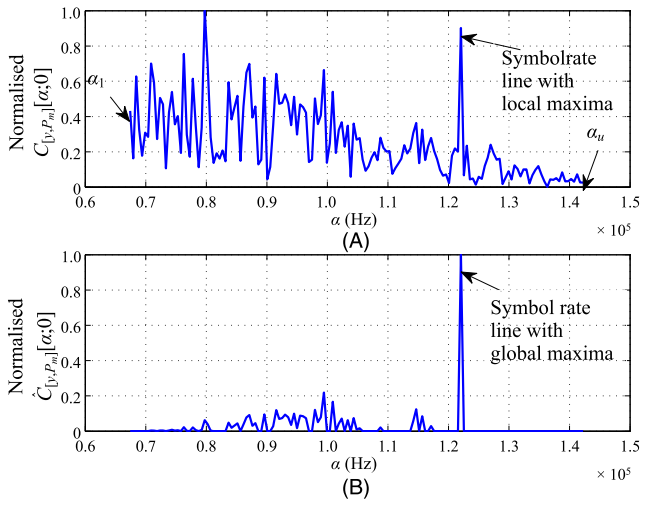

FIGURE 1 (A) NWCS having a symbol rate line as a local maxima at a small roll-off factor ($\beta = 0.2$) and low SNR (5 dB). (B) WCS under the same conditions as Figure 1A converts the local symbol rate line to a global maxima

The Q component is compensated by $P/2$ samples to make the phase difference zero at $\alpha = 1/P$. However, the offset $P/2$ is not known at the receiver; therefore, a set of approximate offsets $\{P_m/2\}_{m=0}^{M-1}$ is used to maximize the cyclic spectrum.

In order to develop the weighting function, we observe the properties of the cyclic spectrum. We find that the noise floor is lower than the amplitude of the symbol rate frequency, so the weighting operation is applied to the cyclic frequency, which has a higher amplitude than the average of the signal strength, $\overline{C}_{[x,P_m]}[\alpha;0]$. We also find that the peak at the symbol rate appears distant from the baseband cyclic components, so weights are assigned proportional to the cyclic frequency, That is, a higher weight is assigned to upper frequencies and a lower weight to lower frequencies. This is achieved by multiplying the weight by α^2.

From the above observations, we weight the cumulant $C_{[x,P_m]}[\alpha;0]$ with the help of an elementary nonlinear process defined as follows:

$$\hat{C}_{[x,P_m]}[\alpha;0] = C_{[x,P_m]}[\alpha;0] + \left(C_{[x,P_m]}[\alpha;0] - \overline{C}_{[x,P_m]}[\alpha;0]\right)\alpha^2. \tag{10}$$

Figure 1 illustrates the effect of the weighting operation. It provides a non-weighted–cyclic spectrum (NWCS) and a normalized weighted-cyclic spectrum (WCS) at a low SNR of 5 dB and a small excess bandwidth signal ($\beta = 0.2$). Figure 1 is supposed to have only one nonzero peak, but owing to the presence of noise, it shows many local peaks. The weighting method applied using (10) converts the local maxima at $\alpha = 1/P$ in Figure 1A to a global maxima in Figure 1B.

Now, we search for the highest cyclic peak by performing a maximization operation of $|\hat{C}_{[x,P_m]}[\alpha;0]|$ over α and P_m, That is,

$$\hat{f}_s = \arg\max_{\alpha,m} |\hat{C}_{P_m}[\alpha;0]|. \tag{11}$$

Figure 2 indicates that the phase curves for WCS and NWCS are identical, so the same STO estimation process is followed for both weighted and unweighted signals. This can also be proven by simplifying (10) as follows. First and foremost, the average amplitude of $C_{P_m}[\alpha;0]$ is calculated as follows:

$$\begin{aligned}\overline{C}_{[x,P_m]}[\alpha;0] &= \sum_{-\infty}^{\infty} \alpha(C_{P_m}[\alpha;0]) \\ &= \sum_{-\infty}^{\infty} \alpha \frac{1}{2P} G\left[\frac{1}{P}\right] e^{-j2\pi N_\tau/P} \left(\sigma_r^2 \delta\left[\alpha - \frac{1}{P}\right]\right. \\ &\quad \left. + \sigma_i^2 \delta\left[\alpha - \frac{1}{P}\right] e^{-j2\pi\alpha(P/2-P_m/2)}\right) \\ &= \frac{1}{2P^2} G\left[\frac{1}{P}\right] e^{-j2\pi N_\tau/P} \left(\sigma_r^2 + \sigma_i^2 e^{\frac{-j2\pi}{P}\left(\frac{P}{2}-\frac{P_m}{2}\right)}\right).\end{aligned} \tag{12}$$

We observe from (12) that the maxima are achieved at $\alpha = 1/P$ when $(P/2 - P_m/2) \to 0$. Hence the above equation can be written as follows:

$$\overline{C}_{[x,P_m]}[\alpha;0]|_{\alpha=1/P} = \frac{1}{2P^2} G\left[\frac{1}{P}\right] e^{-j2\pi N_\tau/P}(\sigma_r^2 + \sigma_i^2). \tag{13}$$

The result of (13) is substituted into (10), which is further simplified as follows:

$$\begin{aligned}&\hat{C}_{[x,P_m]}[\alpha;0]|_{\alpha=1/P} \\ &= \frac{1}{2P} G\left[\frac{1}{P}\right](\sigma_r^2 + \sigma_i^2) e^{-j2\pi N_\tau/P}\left[1 + \frac{1}{P^2} + \frac{1}{P^3}\right].\end{aligned} \tag{14}$$

Thus, the STO is estimated by taking the phase of the above signal as follows:

$$\arg(\hat{C}_{[x,P_m]}[\alpha_k;0]) = -2\pi N_\tau/P.$$

Finally, the estimated symbol timing offset is obtained as follows:

$$\hat{N}_\tau = \frac{-P}{2\pi} \arg(\hat{C}_{[x,P_m]}[\alpha;0])|_{\alpha=1/P}. \tag{15}$$

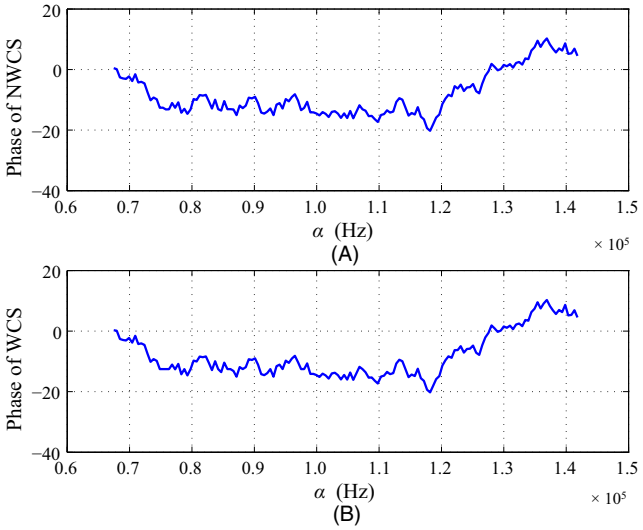

FIGURE 2 (A) Phase plot of NWCS. (B) Phase plot of WCS for the same set of parameters

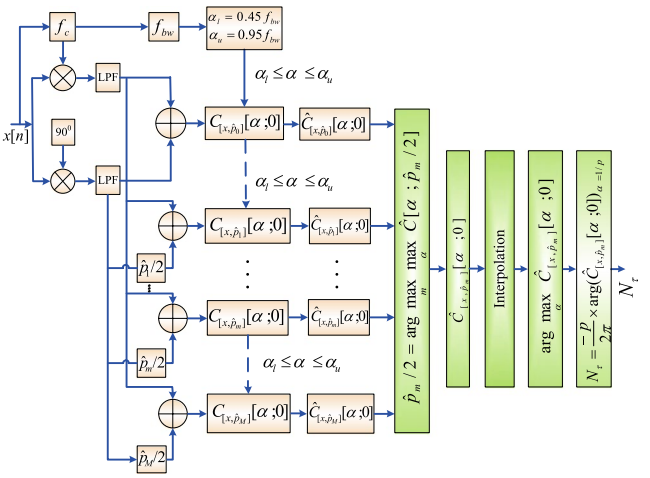

FIGURE 3 Implementation of STO estimation for LMS

It appears that the estimation process is exhaustive and intense searching is required, but from Figure 3, the algorithm can be implemented with the help of parallel cyclic spectrum computation. Therefore, no additional time is required even in the case of a large set of approximate offsets M. Furthermore, the complexity of the estimator is reduced by introducing the search interval $[\alpha_l, \alpha_u]$.

We observe that no information pertaining to carrier phase, frequency offset, or modulation schemes is required for the STO estimation. In the course of computing the second-order cyclic cumulant, examination of (3) and (8) indicates that carrier phase and frequency offset are eliminated by applying the conjugate operation and zero time-lag. Thus, the performance of the proposed blind STO estimation method is robust in the presence of carrier phase and frequency offset, as neither parameter affects the calculation.

4 | RESULTS FROM SIMULATION AND MEASUREMENT

In the following section, the performance of the proposed STO estimation algorithm is assessed by simulation and measurement results. The simulation parameters of the system that have been considered are a receiver sampling rate of 48 MHz; carrier frequency of 5 MHz; oversampling factor of 12; roll-off factor of 0.5; symbol rate of 4 MHz; and the number of symbols is 500. The performance is evaluated over 1000 iterations. The channel considered for simulation results is the Rayleigh flat fading channel.

Although the proposed method is derived for OQPSK modulated signals, the method works for all LMS. Subsequently, we adopt the normalized mean square error (NMSE) as the comparison measure to evaluate the estimation performance of the proposed method at different SNR, which is defined as $E\{(N_\tau - \hat{N}_\tau)^2/N_\tau^2\}$ for the estimated STO, $\hat{N}_\tau$.

Figure 4 plots the NMSE for LMS such as BPSK, QPSK, π/4-QPSK, and 16 QAM, along with OQPSK modulated signals using the proposed method. It is observed that all the modulation schemes yield similar performances. We calculate NMSE values of 2×10^{-5} to 5×10^{-5} at 30 dB SNR, which indicate good estimation performance. The estimated STO is compensated to demodulate the received signal without any offset error in the system.

Figure 5 shows the NMSE plot in the case of OQPSK for different values of timing offsets to evaluate its biasedness. It provides almost the same results for different values of STO, that is, for $N_\tau = 3$, 6, and 8. This implies that the proposed estimator is not biased with respect to the STO present in the signal.

Figure 6 presents the performance comparison between the proposed method and the method proposed in [29] (henceforth referred to as AAU-EST) for OQPSK modulated signals with different values of roll-off factor ($\beta = 0.2$ and 0.75). The number of symbols considered for observation is 500. The proposed STO estimator outperforms the existing AAU-EST method at all SNRs. However, for a high roll-off factor, the dominance of the proposed STO estimator is less marked, as its performance remains almost constant with respect to the roll-off factor, β, because of the weighting operation applied to the cyclic spectrum.

Figure 7 illustrates how the oversampling factor affects the STO estimation performance using different oversampling factors of $P = 6$, 8, 10, and 12. As the oversampling factor increases, the performance of the proposed STO estimation improves because the frequency resolution is proportional to the oversampling factor [36]. However, we cannot enhance the performance by simply increasing the oversampling factor because this introduces memory constraint and complexity issues.

Figure 8 depicts NMSE vs the number of observed symbols when the roll-off factor is $\beta = 0.5$ and the oversampling is $P = 12$ at 15 and 20 dB SNR. The NMSE approaches 2×10^{-4} at 15 dB and 1×10^{-4} at 20 dB after 400 observed symbols.

The computational complexity of the proposed and AAU-EST methods in the upper bound form are $\mathcal{O}(NP \log_2 (KP)))$ and $\mathcal{O}((KP)^2))$, respectively, where P is the oversampling factor and K is the number of symbols. The proposed method has lower complexity compared to the AAU-EST method.

In Figure 9, the received constellation plot of OQPSK is shown with the STO of three samples at 10 dB and 20 dB received SNR.

For the measurement, the same set of simulation parameters is used and we have added an IF carrier frequency of 5 MHz and RF carrier frequency of 2.3 GHz. In the experimental setup, we use the NI PXIe testbed, which is configurable by the software program [37]. In the transmitter, an NI RF signal generator is used to obtain the OQPSK modulated signal, which is passed through the arbitrary function generator and then fed into the local oscillator and then to the RF up-converter to transmit it through the antenna. The signal is received with the help of a specified RF filter span. A

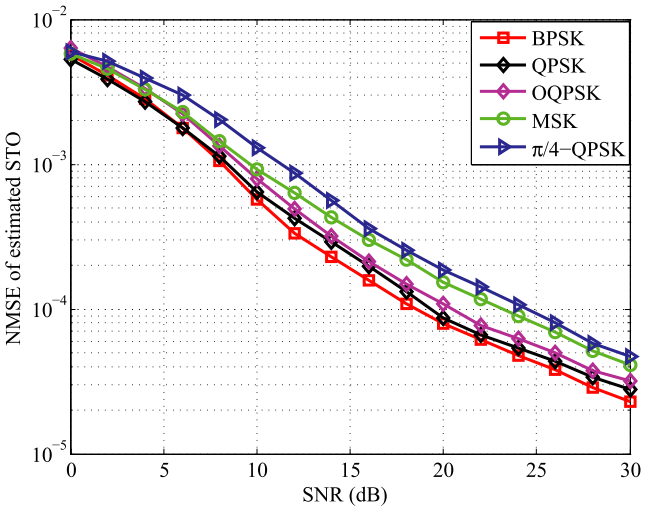

FIGURE 4 NMSE vs SNR for different LMS at $\beta = 0.5$ with 500 symbols

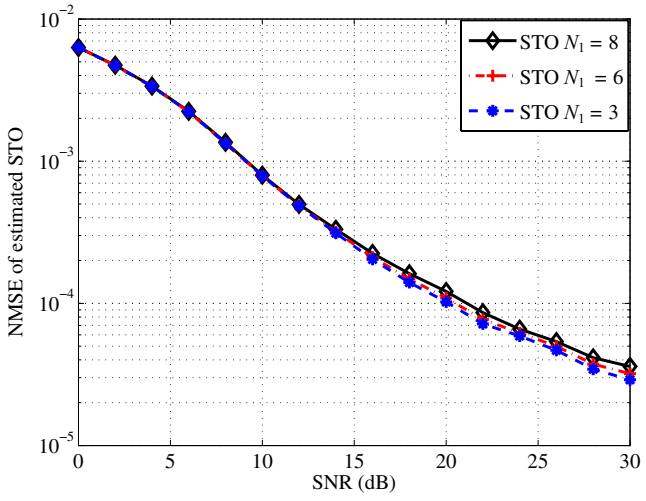

FIGURE 5 NMSE vs SNR for OQPSK with different values of timing offset for $\beta = 0.5$

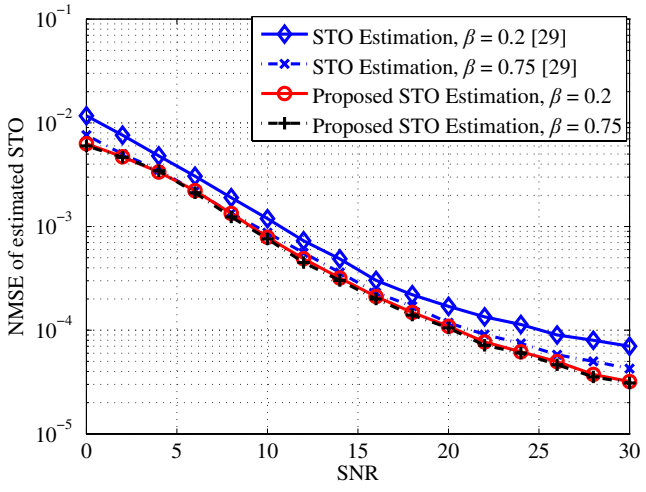

FIGURE 6 NMSE vs SNR comparison between the proposed method and AAU-EST 30 for $\beta = 0.2$ and 0.75

threshold value is predefined, which is calculated as the power of the noise in the absence of a transmitted signal. Then, we compare the power of the received signal with the predefined threshold value. If the power level detected is higher than the threshold value, the RF carrier frequency $\hat{f}_{RF}$ is estimated by observing the peak position of the signal. If the power level does not exceed the threshold, signals are disregarded until a signal with a higher power level than the threshold is detected.

Figure 10 shows the front panel of the configured transmitter setup using PXIe-5673 for OQPSK modulated signals.

In the implementation, the received RF signal of 2.3 GHz is first converted into the IF signal of 5 MHz. The specified frequency of the IF signal is obtained by feeding the local oscillator frequency f_{LO} to the RF down-converter, where the IF carrier frequency is calculated by $f_{IF} = \hat{f}_{RF} - f_{LO}$, where $f_{LO} = \hat{f}_{RF} - 5\,\text{MHz}$, and $\hat{f}_{RF}$ is the estimated RF carrier frequency. As there is a frequency loss of approximately 100 Hz–1500 Hz when the RF is down-converted to IF, the frequency of the received IF signal is only approximately 5 MHz, because $\hat{f}_{RF}$ is not known in advance to the receiver. However, the implementation is not significantly affected by the frequency loss because the IF frequency is estimated from the resultant IF signal. The detailed testbed setup and measurement is presented in [3]. We performed the experimental analysis in the line of sight

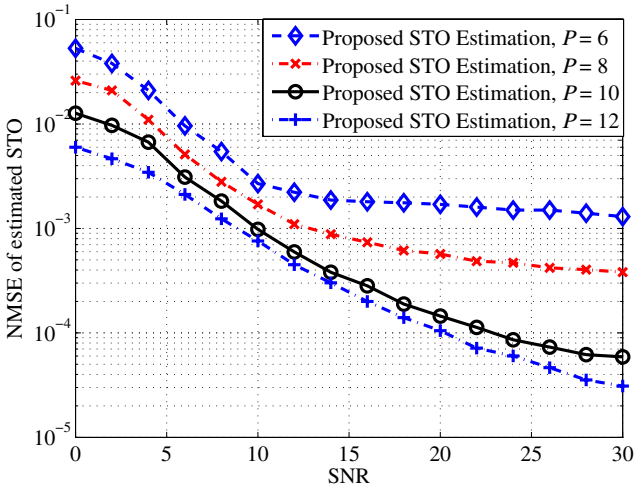

FIGURE 7 Performance evaluation of the proposed method for different values of oversampling factor, $\beta = 0.5$

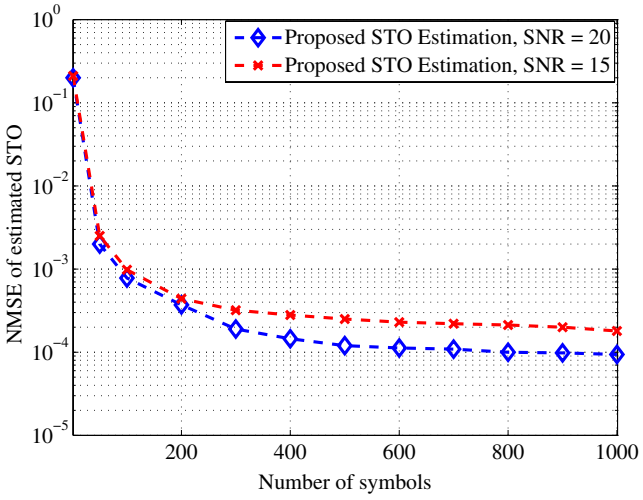

FIGURE 8 NMSE vs number of observed symbols at 15 and 20 dB SNR; oversampling $P = 12$; and roll-off factor $\beta = 0.5$

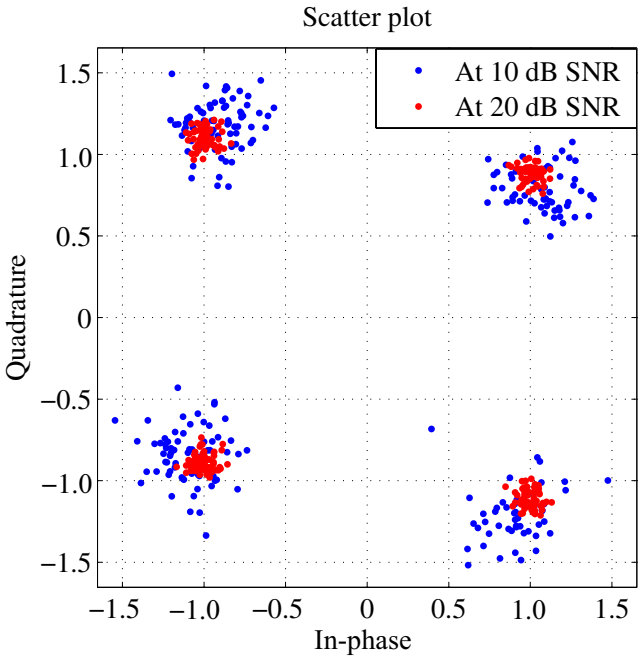

FIGURE 9 Received constellation points for OQPSK signal at 10 dB and 20 dB SNR

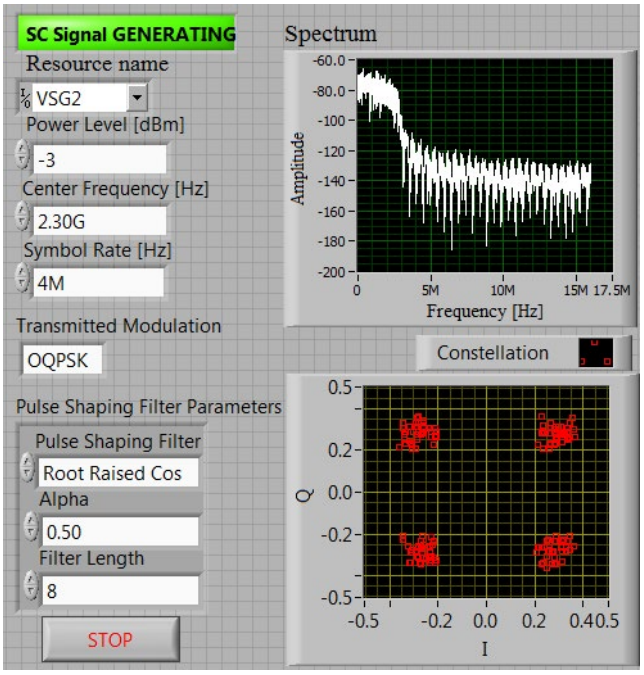

FIGURE 10 Front panel graphical user interface of the transmitter setup using PXIe-5673

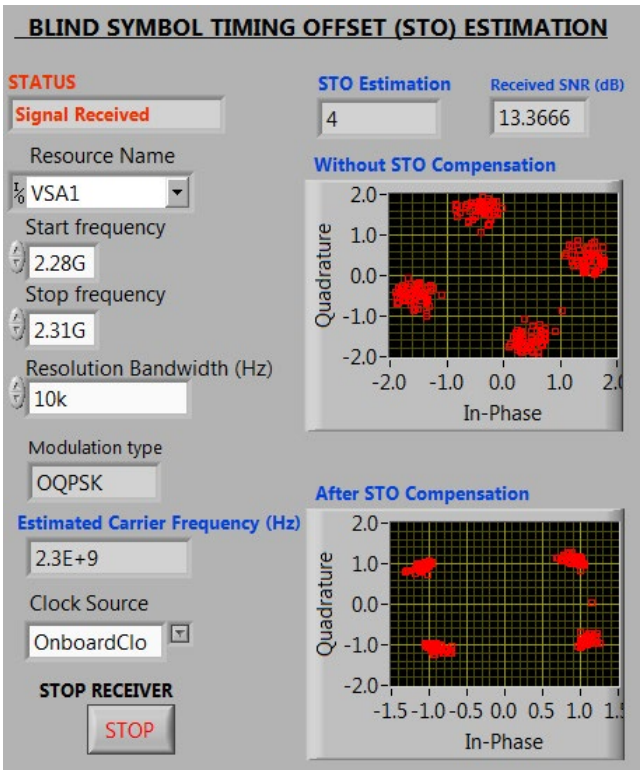

FIGURE 11 Front panel graphical user interface of the receiver setup using PXIe-5663

condition between transmitter and receiver separated by 3 m in an indoor environment; therefore, a flat fading channel condition is created for measurement purposes [38].

Figure 11 presents the front panel of the receiver setup using PXIe-5663, where the STO of four samples is estimated blindly at a 13.37 dB received SNR. The constellation points are provided for the OQPSK modulated signal in the presence of four STO samples and after STO compensation.

5 | CONCLUSION

A new blind STO estimation method has been presented for OQPSK modulated signals, which also works for other LMS. The proposed method compensates the offset between the I and Q components of an OQPSK signal and utilizes the cyclostationarity features of the signal to obtain the phase (STO) at the symbol rate line in the cyclic frequency domain. The proposed scheme uses WCS, which allows for an efficient estimation process, even in cases involving low received SNR or a small roll-off factor. The NMSE values of the STO and constellation points have been plotted to measure the accuracy of the estimation process. Measurement and theoretical studies have been carried out in an indoor environment using a line of sight communication setup and Rayleigh flat fading channel condition. The proposed method exhibits robust performance in the presence of carrier phase offset and frequency offset.

ACKNOWLEDGMENTS

This work was supported in part by the Visvesvaraya Young Faculty Research Fellowship, Ministry of Electronics and Information Technology, Government of India, being implemented by the Digital India Corporation and Early Career Young Scientists by the Science and Engineering Research Board under the Department of Science and Technology, Government of India, and in part by the Natural Sciences and Engineering Research Council of Canada through its Discovery Program.

ORCID

Sushant Kumar https://orcid.org/0000-0003-1815-6647

REFERENCES

1. S. Majhi and T. S. Ho, *Blind symbol-rate estimation and testbed implementation of linearly modulated signals*, IEEE Trans. Veh. Technol. **64** (2015), no. 3, 954–963.
2. S. Majhi, M. Kumar, and W. Xiang, *Implementation and measurement of blind wireless receiver for single carrier systems*, IEEE Trans. Instrum. and Meas. **66** (2017), no. 8, 1965–1975.
3. S. Majhi et al., *Hierarchical hypothesis and feature-based blind modulation classification for linearly modulated signals*, IEEE Trans. Veh. Technol. **66** (2017), no. 12, 11057–11069.
4. M. Jo et al., *Selfish attacks and detection in cognitive radio ad-hoc networks*, IEEE Netw. **27** (2013), no. 3, 46–50.
5. B. Uengtrakul and D. Bunnjaweht, *A cost efficient software defined radio receiver for demonstrating concepts in communication and signal processing using python and RTL-SDR*, in Proc. Int. Conf. Digital Inf. Commun. Technol. its Applicat., Bangkok, Thailand, 2014, May 2014, pp. 394–399.
6. K. Choi and H. Liu, *QPSK and offset QPSK in Simulink*, Problem-Based Learning in Communication Systems Using MATLAB and Simulink, IEEE, Piscataway, NJ, 2016, pp. 239–253.
7. D. Raphaeli, *A reduced complexity equalizer for OQPSK*, IEEE Trans. Commun. **58** (2010), no. 1, 46–51.
8. J. Nsenga et al., *Spectral regrowth analysis of band-limited offset-QPSK*, in Proc. IEEE Int. Conf. Acoustic, Speech Signal Process., Lasvegas, NV, USA, Mar. 2008, pp. 3593–3596.
9. T. F. Detwiler et al., *Offset QPSK receiver implementation in 112 Gb/s coherent optical networks*, in Proc. Eur. Conf. Exhibition Optical Commun., Torino, Italy 2010, pp. 1–3.
10. K. Vasudevan, *Synchronization of bursty offset QPSK signals in the presence of frequency offset and noise*, in Proc. TENCON-IEEE Region 10, Conf., Hyderabad, India, Nov. 2008, pp. 1–6.
11. X. Man et al., *Improved code-aided symbol timing recovery with large estimation range for LDPC-coded systems*, IEEE Commun. Lett. **17** (2013), no. 5, 1008–1011.
12. J. S. Baek and J. S. Seo, *Effective symbol timing recovery based on pilot-aided channel estimation for MISO transmission mode of DVB-T2 system*, IEEE Trans. Broadcast. **56** (2010), no. 2, 193–200.
13. Z. Shen et al., *ML-based iterative sequence estimation without symbol timing recovery*, IEEE Commun. Lett. **17** (2013), no. 10, 2004–2007.

14. G. Vazquez and J. Riba, *Signal processing advances in wireless and mobile communications*, non-data-aided digital synchronization, ch. 9, 2000.
15. Y. Chi, L. Chen, and C. Lv, *A symbol timing recovery algorithm of M-PSK signals for burst modem applications with small packet size*, China Commun. **13** (2016), no. 6, 138–146.
16. B. A. Bhatti et al., *Carrier and symbol synchronization in digital receivers using feedback compensation loop and early late gate on FPGA*, in Proc. Int Conf. Robotics Emerging Allied Technolo. Eng., Islamabad, pakistan, Apr. 2014, pp. 146–150.
17. P. Shachi, R. Mishra, and R. K. Jatoth, *Coherent BPSK demodulator using costas loop and early-late gate synchronizer*, in Proc. Int. Conf. Comput., Commun. Netw. Technol., Tiruchengode, India, July 2013, pp. 1–6.
18. K. Gorantla and V. V. Mani, *Synchronization in IEEE 802.15.4 Zigbee transceiver using Matlab simulin*, in Proc. Int. Conf. Adv. Comput. Commun. Inf., Kochi, India, Aug. 2015, pp. 144–148.
19. K. Mueller and M. Muller, *Timing recovery in digital synchronous data receivers*, IEEE Trans. Commun. **24** (1976), no. 5, 516–531.
20. F. Gardner, *A BPSK/QPSK timing-error detector for sampled receivers*, IEEE Trans. Commun. **34** (1986), no. 5, 423–429.
21. D. Lim, *A modified Gardner detector for symbol timing recovery of M-PSK signals*, IEEE Trans. Commun. **52** (2004), no. 10, 1643–1647.
22. M. Oerder and H. Meyr, *Digital filter and square timing recovery*, IEEE Trans. Commun. **36** (1988), no. 5, 605–612.
23. M. Rahnema, *Symbol timing recovery algorithms and their evaluation for burst communication*, Int. J. Wireless Inf. Netw. **5** (1988), no. 4, 341–350.
24. F. Gini and G. B. Giannakis, *Frequency offset and symbol timing recovery in flat-fading channels: a cyclostationary approach*, IEEE Trans. Commun. **46** (1998), no. 3, 400–411.
25. J. Wang and J. Speidel, *16-QAM symbol timing recovery in the upstream transmission of DOCSIS standard*, IEEE Trans. Broadcast. **49** (2003), no. 2, 211–216.
26. T. Fusco and M. Tanda, *Blind feedforward symbol-timing estimation with PSK signals: a constant-modulus approach*, IEEE Trans. Commun. **55** (2007), no. 2, 242–246.
27. D. A. Gudovskiy, L. Chu, and S. Lee, *A novel nondata-aided synchronization algorithm for MSK-type-modulated signals*, IEEE Commun. Lett. **19** (2015), no. 9 1552–1555.
28. J. A. Lopez-Salcedo and G. Vazquez, *Cyclostationary joint phase and timing estimation for staggered modulations*, in Proc. IEEE Int. Conf. Acoustics, Speech, Signal Process., Montreal, Canada, May 2004, pp. 833–836.
29. A. A. D'Amico, A. N. D'Andrea, and U. Mengali, *Feedforward joint phase and timing estimation with OQPSK modulation*, IEEE Trans. Veh. Technol. **48** (1999), no. 3, 824–832.
30. M. Moeneclaey and G. Ascheid, *Extension of the Viterbi and Viterbi carrier synchronization algorithm to OQPSK transmission*, in Proc. Int. Workshop DSP Applied Space Commun., Torino, Canada, Sept. 1990.
31. W. A. Gardner (ed.), *An introduction to cyclostationary signals, chapter 1*, Cyclostationarity in Communications and Signal Processing IEEE Press, New York, 1994, pp. 1–90.
32. A. V. Dandawate and G. B. Giannakis, *Statistical test for presence of cyclostationarity*, IEEE Trans. Signal Process. **42** (1994), no. 9, 2355–2369.
33. G. Zhou and G. B. Giannakis, *Harmonics in multiplicative and additive noise: Performance analysis of cyclic estimator*, IEEE Trans. Signal Process. **43** (1995), no. 9, 2217–2221.
34. S. Majhi, C. Yading, and S. H. Ting, *Design and implementation of a universal receiver testbed for single carrier and multicarrier signals on NI PXIe platforms*, National Instruments ASEAN Graphical System Design Achievement Awards, Sept. 2012.
35. P. Ciblat et al., *Asymptotic analysis of blind cyclic correlation-based symbol-rate estimators*, IEEE Trans. Inf. Theory **48** (2002), no. 7, 1922–1934.
36. M. Flohberger et al., *Symbol rate estimation with inverse fourier transforms*, in Proc. Int. Workshop Satellite Space Commun., Madrid, Spain, Sept. 2006, pp. 110–113.
37. National Instruments PXI platform, Banglore, India, http://www.ni.com/pxi/.
38. T. S. Rappaport, *Wireless communications: Principles and practice*, 2nd edition, Prentice Hall PTR, Dec. 2002.

AUTHOR BIOGRAPHIES

Sushant Kumar received his B.Tech. degree in Electronics and Communication from ICFAI University, Dehradun, India, in 2011, and his M.Tech. degree in Communication System Engineering from the Indian Institute of Technology, Patna, India, in 2015. He is currently working toward his PhD degree in Electrical Engineering from the Indian Institute of Technology, Patna, India. His research interests include signal processing, wireless communication, and timing and frequency synchronization in SC-FDMA and MIMO SC-FDMA.

Sudhan Majhi is an Associate Professor with the Department of Electrical Engineering, Indian Institute of Technology, Patna, India. Currently, he is a Fellow of Sir Visvesvaraya Young Faculty Research. He received his M.Tech. degree in Computer Science and Data Processing from the Indian Institute of Technology, Kharagpur, India, in 2004 and his PhD degree from Nanyang Technological University, Singapore, in 2008. He has postdoctoral experience at the University of Michigan-Dearborn, MI, USA, Institute of Electronics and Telecommunications, Rennes, France, and Nanyang Technological University, Singapore. His research interest is in signal processing for wireless communication, which includes blind synchronization and parameter estimation, cooperative communications, physical layer security for cognitive radio, sequence design, OFDM, MIMO, SC-FDMA, and MIMO-OFDM.